

LA-UR-13-20254

Approved for public release; distribution is unlimited.

Title: MCNP Simulations of Background Particle Fluxes from Galactic Cosmic Rays

Author(s): Palomares, Javier
McKinney, Gregg W.

Intended for: ANS Annual Meeting, 2013-06-16/2013-06-20 (Atlanta, Georgia, United States)



Disclaimer:

Los Alamos National Laboratory, an affirmative action/equal opportunity employer, is operated by the Los Alamos National Security, LLC for the National Nuclear Security Administration of the U.S. Department of Energy under contract DE-AC52-06NA25396. By approving this article, the publisher recognizes that the U.S. Government retains nonexclusive, royalty-free license to publish or reproduce the published form of this contribution, or to allow others to do so, for U.S. Government purposes. Los Alamos National Laboratory requests that the publisher identify this article as work performed under the auspices of the U.S. Department of Energy. Los Alamos National Laboratory strongly supports academic freedom and a researcher's right to publish; as an institution, however, the Laboratory does not endorse the viewpoint of a publication or guarantee its technical correctness.

MCNP Simulations of Background Particle Fluxes from Galactic Cosmic Rays

J. Palomares¹, G. W. McKinney²,

(1) Stanford University, P.O. Box 11620, Stanford, CA, 94305; javierp@stanford.edu

(2) Los Alamos National Laboratory, P.O. Box 1663 MS C921, Los Alamos, NM, 87545; gwm@lanl.gov

INTRODUCTION

Recently, a new galactic cosmic-ray (GCR) source option [1] was implemented in the all-energy, all-particle transport code MCNP6 [2]. In this paper, we made use of this feature to calculate surface neutron and photon background fluxes on a terrestrial grid around the earth. These spectra have been incorporated into Release 2 of the “background.dat” file, which is read and sampled by MCNP6 whenever a user invokes the background source option [2].

Cosmic radiation bombards Earth with various particles, such as protons and α particles, some of which are deflected by the Earth’s shielding magnetic field. Particles that carry sufficient energy can overcome the deflection and penetrate into the atmosphere. The sufficient energy is dependent on the terrestrial coordinates due to the magnetic force’s proportionality to the sine of the angle between the velocity vector of the incoming particle and the magnetic field.

As the particles propagate through the atmosphere, collisions with atmospheric molecules generate new particles such as neutrons, protons, photons, muons, pions, and other exotic particles. These secondary particles often have sufficient energy to undergo additional nuclear interactions, and so on, forming what is known as a cascade shower.

The tabulation of background particle fluxes on the surface of the earth is important for a variety of reasons, one of which is the design of nuclear material detection systems.

DESCRIPTION OF THE ACTUAL WORK

The simulations reported here used various models and formulations for the cosmic source spectra, atmosphere, and terrestrial conditions to correctly model the propagation of GCR particles through the atmosphere to surface level.

Cosmic Source Spectra

MCNP provides two different formulations of GCR spectra: an older formulation, referred to as LEC (Lal with Energy Cutoffs), proposed by the Physical Research Laboratory (Ahmedabad, India) [3], and a modern formulation developed at the Bartol Research Institute (BRI, University of Delaware, Newark, DE) in 2004 [4]. LEC uses a known analytical form for the differential 4π GCR flux spectrum. The BRI formulation uses evaluated

“sky-maps” that describe terrestrial spatial (longitude, latitude, altitude) and angular (polar, azimuthal) dependence of GCR rigidity (energy spectrum) cutoff values resulting from modulation from terrestrial magnetic shielding. Sample proton spectra produced by these two formulations are shown in Figs. 1 and 2 for minimum and maximum solar modulation. Whenever a user specifies a terrestrial location (via the LOC keyword), the BRI formulation is invoked, providing automatic normalization of the source and Monte Carlo sampling of light and heavy GCR (although in the current version of MCNP6 only protons and alphas are utilized).

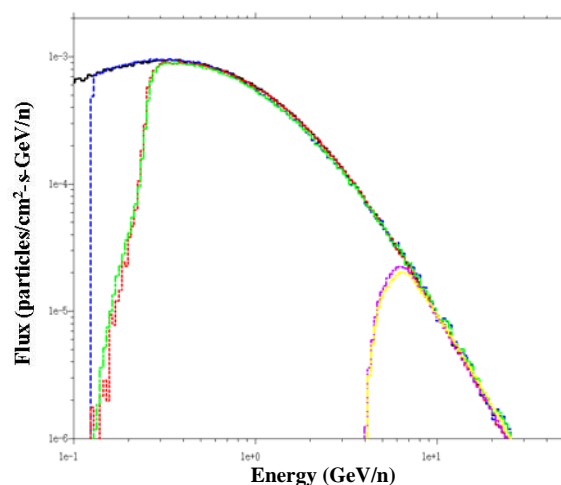


Fig. 1. Proton spectra for minimum solar modulation (1987) at 80°N, 120°W (black=LEC, blue=BRI), 53°N, 120°W (red=LEC, green=BRI), and 32°N, 120°W (purple=LEC, yellow=BRI).

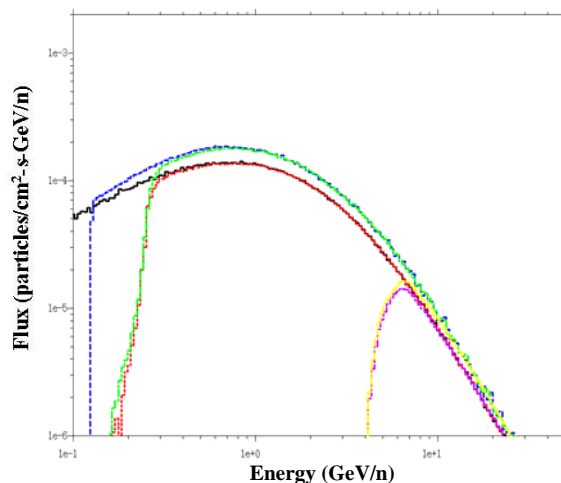


Fig. 2. Proton spectra for maximum solar modulation (1981) at 80°N, 120°W (black=LEC, blue=BRI), 53°N, 120°W (red=LEC, green=BRI), and 32°N, 120°W (purple=LEC, yellow=BRI).

MCNP models solar modulation by interpolation of measured data (1965-2005) or parameterized data (for years outside the range), using a specified date (via the DAT keyword) and a standard formulation [5]. It models geomagnetic modulation by truncating the energy sampling spectrum of protons and α particles in accordance to the BRI rigidity cutoff as previously described.

Atmosphere Model

These simulations modeled the atmosphere as a rectangular prism protruding from 2 meters below sea level up to 65 km in altitude with a base of 200m by 200m. The prism was segmented horizontally into 300 cells to account for the varying atmospheric conditions (temperature, pressure, air composition). Temperature (T) and pressure (p) altitude profiles were taken from the U.S. Standard Atmosphere [6]:

$$T = T_0 - L h$$

$$p = p_0 (1 - L h / T_0)^{g M / (R L)},$$

with the parameters described in the following table.

Physical Quantity	Value
Sea Level Temperature, T_0	288.15 K
Sea Level Pressure, p_0	$1.01325 \cdot 10^5$ Pa
Temperature Lapse Rate, L	.0065 K/m (altitude dependent)
Altitude, h	
Air Molar Mass, M	28.9644 g/mol
Gravity, g	9.80665 m/s^2
Gas Constant, R	8.315 J/(K mol)

Atmospheric density was computed from the Ideal Gas Law,

$$\rho = p M / (R T).$$

Air composition was defined by the standard fractions ($n_N = .78$ for nitrogen, $n_o = .21$ for oxygen, and $n_{Ar} = .01$ for argon) for high atmosphere, and allowed to contain water vapor near the ground according to a specified relative humidity (RH). The hydrogen fraction content of air was determined by

$$n_H = RH p_s / p,$$

where p_s is the saturated vapor pressure given by the Arden-Buck equation (p_s in kPa and T in $^{\circ}\text{C}$),

$$p_s = 6.1121 e^{((18.678 - T/234.5)/(T + 257.14 + T))}.$$

This result is then normalized by dividing over the sum of total elemental fractions to give the hydrogen atomic fraction, or

$$A_H = 2n_H / (2n_o + n_{Ar} + 2n_N + 2n_H).$$

A_H is multiplied by the atomic mass of hydrogen and once again normalized to give the final mass fraction. The oxygen fraction increases modestly from the humidity,

$$A_o = (2 * n_o + n_H) / (2n_o + n_{Ar} + 2n_N + 2n_H).$$

However, initial results indicate that relative humidity does not have a significant impact on the ground-level neutron flux, and subsequent simulations were all set to a relative humidity of 50 % (see Fig. 3).

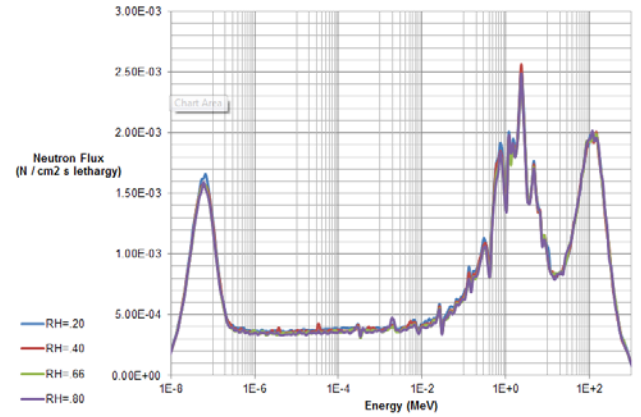


Fig. 3. Neutron lethargy plot for various relative humidities. Results indicate a negligible dependence of the neutron flux on relative humidity. The photon flux also showed little fluctuation with RH.

The average temperature at a terrestrial location [7] was incorporated into the atmospheric conditions by altering the density, temperature profiles, and air compositions.

The density profile was taken from an atmosphere model developed by John Clem [4], which is based on the U.S. Standard Atmosphere [6]. This profile and fits to it are provided in Fig. 4.

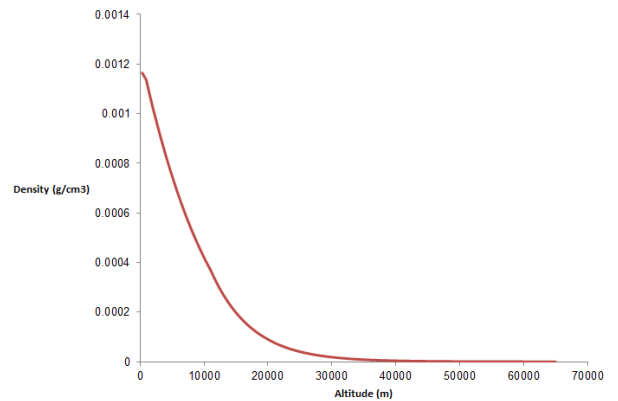


Fig. 4. Air density altitude profile, which is best fit by: $\rho = 1.21e-3 - 9.37e-8 * h$ for $h < 5000\text{m}$ in altitude and $\rho = 1.57e-3 * \exp(-1.45e-4 * h)$ for $h > 5000\text{m}$.

Sea and Ground Models

Similarly, varying ground compositions did not lead to significant changes in the ground-level neutron flux (see Fig. 5), and therefore the ground across all the simulations was taken to be nominal soil [8] (see Table 1). The elevation at a specific terrestrial location was taken into consideration by having the ground cell go from 2 meters below sea level to the terrestrial location's elevation. The atmospheric cells would then follow above that. The terrestrial elevation was obtained using Google Maps' Find Altitude feature [9].

Cases over the ocean were modeled with standard sea water composition (see Table 2). In these cases, the sea water cell went from 2 meters below sea level to sea level.

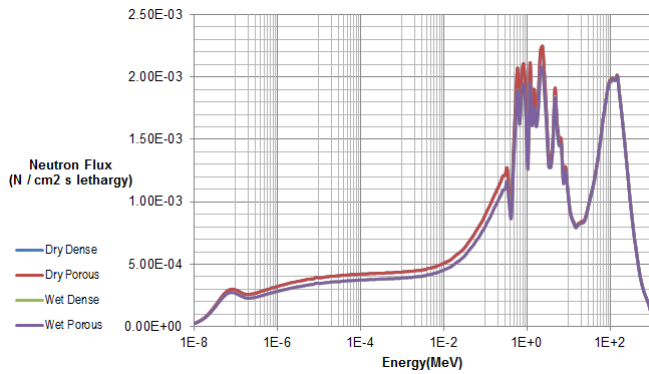


Fig. 5. Neutron Lethargy plot for various ground compositions. 4 different types of soil were tested (dry dense, dry porous, wet dense, wet porous) [8]. The variations of the neutron flux were deemed to be negligible. These results also showed little change in the photon flux spectra.

Table I. Nominal soil composition, with elemental compositions given as mass fractions.

	Nominal
Porosity ^a	0.5
Free water content ^b	0.2
Bound water content ^c	0.05
Mineral density (g/cm ³) ^d	2.684
In situ density (g/cm ³)	1.6104
Element	
Hydrogen	0.02331
Oxygen	0.55921
Silicon	0.22259
Aluminum	0.06528
Iron	0.04015
Calcium	0.02915
Potassium	0.02080
Sodium	0.02272
Magnesium	0.01678

a - Fraction of total volume occupied by water and air

b - Ratio of free water to mineral mass

c - Ratio of bound water to mineral mass

d - Mineral density includes bound water

Table II. Sea water composition, with elemental compositions given as mass fractions. The density is 1.027 g/cm³.

Element	Seawater
Hydrogen	.108211146
Carbon	2.80029*10 ⁻⁵
Oxygen	0.858488424
Chlorine	0.019401998
Sodium	0.010801113
Magnesium	0.001292133
Sulfur	0.000910094
Carbon	0.000400041
Potassium	0.000400041
Bromine	6.70069*10 ⁻⁵

Simulation Details

The GCR source was positioned at the top of the atmosphere (65km) and was specified to produce particles with velocity vectors that have a cosine-squared distribution relative to the surface normal. Reflecting boundaries were specified at the vertical walls of the prism to simulate particles coming in through the atmosphere at off angles.

The background particle flux was computed at 614 terrestrial locations, every 10° in latitude (90°N,80°N, 70°N,...) and longitude (180°W, 170°W, 160°W,...). The flux at each terrestrial location was computed individually.

The simulations ran one million GCR incoming particles for each terrestrial location. The photon and neutron flux across the lowest air cell, from ground level to 2 meters above ground, was tallied and properly normalized.

RESULTS

The MCNP6 simulations were benchmarked by comparing the ground-level neutron flux to measured data taken in 2006 at SNLL (Livermore, CA). As one can see in Fig. 6, the simulation results are ~25% high due to the fact that the nearest simulation grid point was 40°N, 120°W which is ~250 miles NE of Livermore at an elevation of ~5000 feet. Correcting for this difference in elevation gives excellent agreement with the measured data.

These 614 simulations provided ground/sea-level flux spectra for neutrons and protons at each terrestrial location. Fig. 7 and Fig. 8 indicate the variation in these spectra for various locations on Earth.

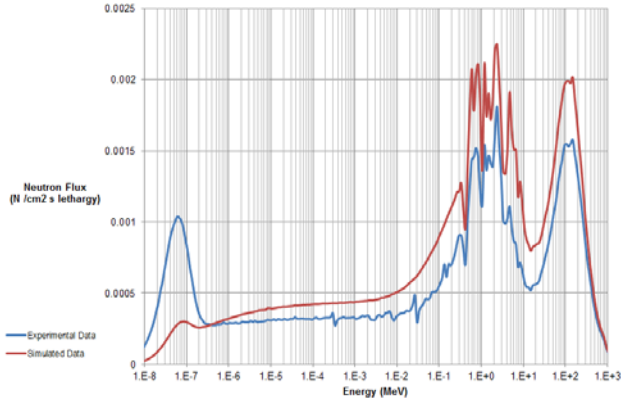


Fig. 6. Benchmark results for the nearest simulation grid-point (40°N , 120°W). Simulation results are high due to the elevation of this grid-point (~ 5000 feet) compared to that of the measured data (~ 500 feet).

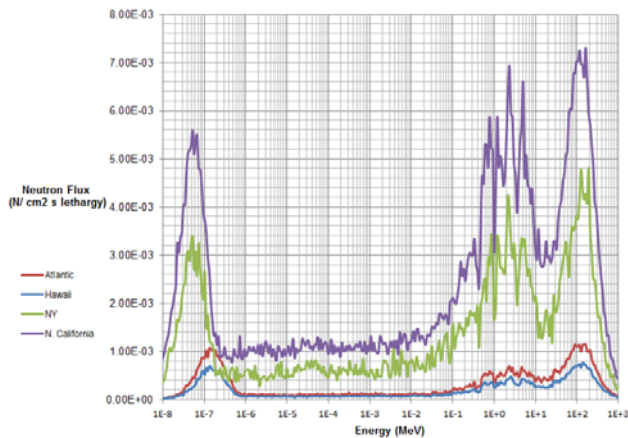


Fig. 7. Neutron differential spectra for four locations: northern California (40°N 120°W , elevation 5000 feet), western Pennsylvania (40°N 80°W , elevation 1000 feet), near Hawaii (20°N 160°W), and in the middle of the Atlantic Ocean (30°N 40°W).

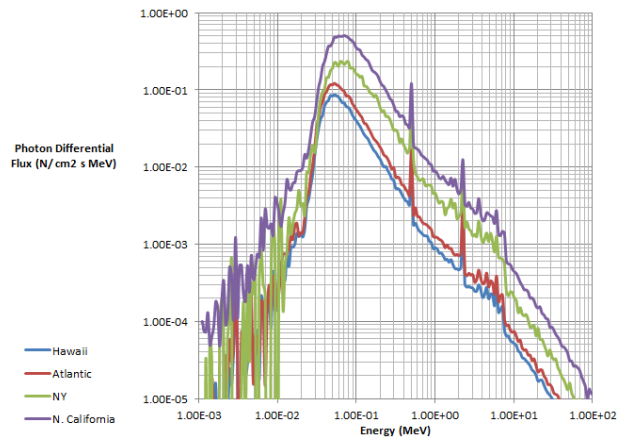


Fig. 8. Photon differential spectra for the locations specified in Fig. 7.

CONCLUSIONS

MCNP was used to produce ground/sea-level neutron and photon cosmic background fluxes on a terrestrial grid

around the earth. These spectra have been incorporated into Release 2 of the “background.dat” file which will be included with the first Production Version of MCNP6 (scheduled for release in spring of 2013). Although the statistical uncertainty of these simulated spectra are a bit high (typically $\sim 20\%$) in the Release 2 data, future releases will include refinements in the statistical errors, geographic gridding, and air density profiles.

ENDNOTES

This work was sponsored by the US Department of Homeland Security, Domestic Nuclear Detection Office, under competitively awarded contract/IAA HSHQDC-12-X-00251. This support does not constitute an express or implied endorsement on the part of the Government.

REFERENCES

1. G. W. MCKINNEY, “MCNP6 Cosmic-Source Option,” Proceedings of ANS Annual Meeting, Chicago, IL, June 24-28 (2012).
2. D. B. PELOWITZ, editor, “MCNP6 User’s Manual, Beta Release” LANL report LA-CP-11-1708 (2011).
3. G. C. CASTAGNOLI and D. LAL, “Solar Modulation Effects in Terrestrial Production of Carbon-14,” *Radiocarbon*, **22**, No. 2, 133-158 (1980).
4. J. M. CLEM, G. DE ANGELIS, P. GOLDHAGEN, and J. W. WILSON, “New Calculations of the Atmospheric Cosmic Radiation Field – Results for Neutron Spectra,” *Radiation Protection Dosimetry*, **110**, pp. 423-428 (2004).
5. G. C. CASTAGNOLI and D. LAL, “Solar Modulation Effects in Terrestrial Production of Carbon-14,” *Radiocarbon*, **22**, No. 2, 133-158 (1980).
6. “U.S. Standard Atmosphere,” NOAA report NOAA-S/T 76-1562, Washington, D.C. (1976).
7. URL <http://colli239.fts.educ.msu.edu/1990/12/31/air-temp-map-1990>.
8. S. L. SHUE, “Fast neutron Thermalization and Capture Gamma-Ray Generation in Soils,” Proceedings of the HSRC/WERC Joint Conference on the Environment, May (1996).
9. URL <http://www.daftlogic.com/sandbox-google-maps-find-altitude.htm>.